Effects of shaft supporting structure on performance test of axial flow fan

R Ma[1], S L Liu[2], M X Li[3], S Y Zheng[1]

[1]Institute of Chemical Machinery, Zhejiang University, Hangzhou, China
[2]School of Mechanical and Automotive Engineering, Zhejiang University of Science and Technology, Hangzhou, China
[3]Department of Mechanical Engineering, Zhejiang University, Hangzhou, China

E-mail: zhengshuiying@zju.edu.cn

Abstract. CFD numerical simulation combined with theoretical analysis are used to research and discuss the obstructing effect, caused by the supporting structure of torsion meter and connecting shaft, on the outlet airflow of axial-flow fan in type-C ducted inlet device. The relations between axial flow fan's total pressure efficiency and flow rate are studied when the distance between supporting structure and outlet section is different, which may provide a reference for the proper design of the performance test device.

1. Introduction

All the ventilation fans have characteristic parameters and performance curves that are acquired through performance test when they leave factory, therefore, fan performance test is an indispensable part of design, production and inspection of fans and device of fan performance test is widely used in various factories and some ancillary departments. At present, the domestic standard of fan performance test is GB1236-2000 'Industrial fans–Performance testing using standardized airways', its technical content and writing rules are equal to ISO 5801: 1997. According to the standard, in the performance test conducted in standardized airways, the input power to the fan shaft needs to be measured when the fan is not directly driven by motor, and it can be measured by using reaction dynamometer or torsion meter. By both means, a supporting structure is needed to support the reaction dynamometer or the torsion meter. In addition, the fan and the torsion meter are connected by shaft which needs to be supported by bearing. If a fan performance test is conducted in a type-C device, the supporting structure of shaft and torsion meter is at the free end of fan outlet, which may obstruct the outflow. According to GB1236-2000, of which section 19.3 specify that 'Care should be taken to avoid the presence of any obstruction which might significantly modify the air flow at inlet or outlet. In particular, no wall or other major obstruction should be closer than 2D from the inlet and 5D on the outlet of the airways or the test fan'[1]. So it is necessary to study the influence of the distances between supporting structure and outlet section on fan performance test. This problem may be frequently encountered in the performance test conducted in type-C device, and related materials are not found at present.

In this paper, CFD numerical simulation[2-4] combined with theoretical analysis are used to research and discuss the obstructing effect of the supporting structure, which may provide a theoretical reference for the edit of fan performance test standard.

2. Model

2.1. Geometry and mesh

The device of fan performance test is type-C with ducted inlet and free outlet, which is composed of bellmouth inlet, flow regulating valve, airway, flow straightener, torsion meter, motor, connecting shaft and fan etc, as shown in figure 1.

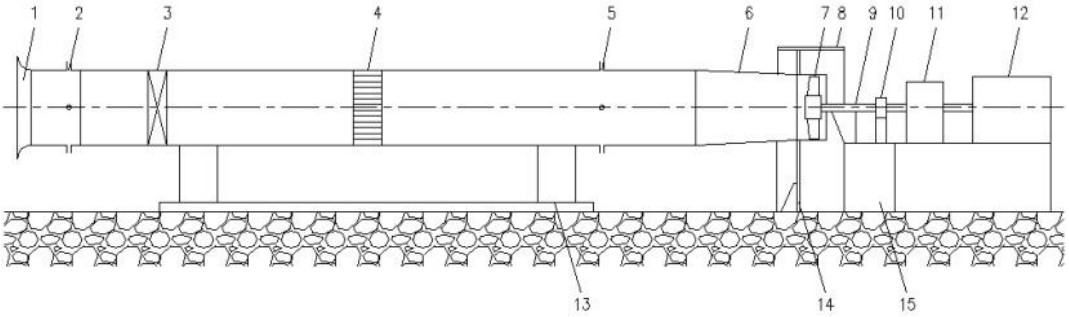

Figure 1. Schematic diagram of performance test device.
1-bellmouth inlet 2-differential pressure tapping 3-flow regulating valve 4-flow straightener 5-static pressure tapping 6-transition duct 7-aixal flow fan 8-protective shield 9-connecting shaft 10-torsion meter 11-high-speed gearbox 12-motor 13-supporting seat of airway 14-vertical plate 15-motor base

The diameter of airway is 700mm. The axial-flow fan has 8 blades. The hub and tip diameter for the rotor is 320mm and 690mm respectively with the hub ratio of 0.46. The shaft diameter is 110mm and the length of fan casing is 200mm. The width of the supporting structure is 50mm and that of the motor base is 200mm.

The computational model is established according to the structure shown in figure 1. It is properly simplified that pressure tapping, flow regulating valve and flow straightener are neglected[5]. Flow rate can be directly specified in CFD commercial software. The computational domain is divided into three parts: inlet region, compeller region and outlet region. The inlet region is the airflow field between static pressure tapping and fan inlet, which is three times the length of airway diameter. The outlet region is the airflow field surrounded by protective shield, and the size is 570mm ×1280mm × 1940mm.

The supporting structure of connecting shaft and motor would inevitably affect the pressure of the airflow at outlet, and further affect the testing efficiency results. So it is necessary to reasonably design the shaft supporting structure and find an appropriate distance between it and fan outlet. Building computational models when this distance is different, and structure diagram along with 3-D model of the computational domain are shown in figure 2. The value of L in figure 2(a) is the distance between shaft supporting structure and fan outlet. To compare with the situation that the fan outlet is not obstructed, the computational model without any supporting structure is established, as shown in figure 2(b).

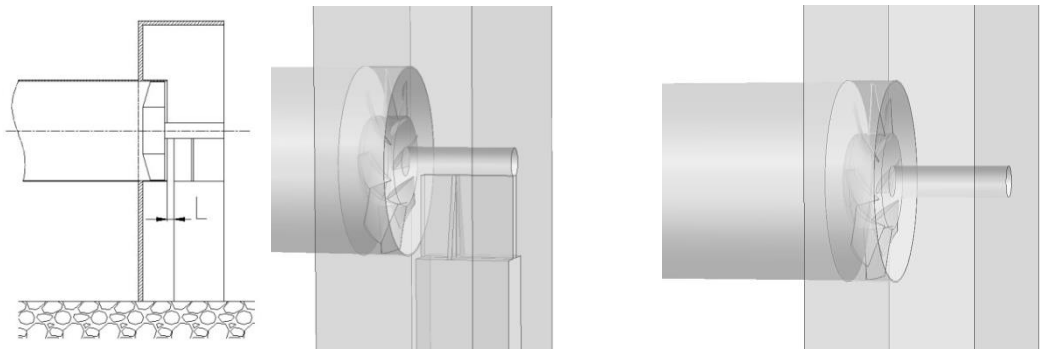

(a) Fan outlet with shaft support **(b)** Fan outlet without shaft support

Figure 2. 3-D model of computational domain.

The modeling process is completed in Turbo module of GAMBIT[6]. Contour lines of the 5 airfoil sections are generated first, and surfaces of the rotor blade are constructed through these contour lines. With these surfaces, we can further stitch out body of the blade and carry out some Boolean operations to create the final computational fluid domain. Impeller model is shown in figure 3.

Structured hexahedral grids are applied in the inlet region with size of 30mm and unstructured tetrahedral grids are applied in the outlet region with size of 20mm. Due to the complexity of blade geometry, tetrahedral meshes are used around the blade with size of 10mm, in terms of the balance of calculation accuracy and computation time. EquiSize Skew of the elements is controlled within 0.9 and the total number of grids is about 2×10^6. The mesh of computational domain is presented in figure 4.

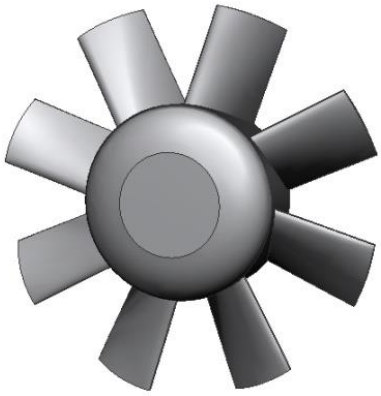

Figure 3. Geometric model of impeller.

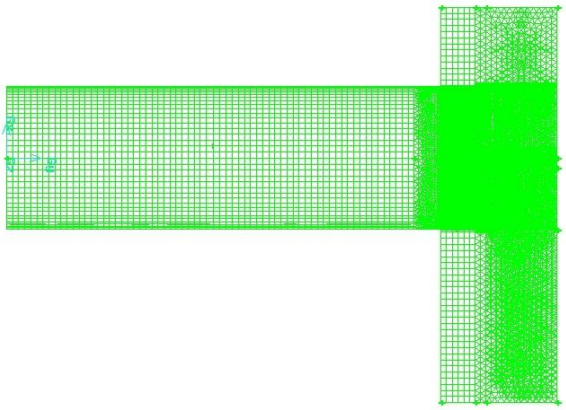

Figure 4. Mesh of computational domain.

2.2. Parameter setting

Following basic assumptions are made: the flow field is taken as three-dimensional steady turbulent flow and the heat conduction problem is neglected, as well as the compressibility of the air. Standard $k-\varepsilon$ turbulence model is enabled. The boundary conditions near the solid walls are analyzed using the method of standard wall function. The coupling equations of pressure and velocities are solved with the SIMPLE algorithm[7]. The numerical simulation of this model was analyzed through first-order upwind difference scheme. Convergence criterion for the equations is 10^{-4}.

The inlet flow uses mass flow rate boundary condition and the velocity direction is normal to boundary. The outlet flow uses pressure boundary condition and the static pressure equals to zero. No-slip boundary condition and multiple reference frame model (MRF) are employed in the simulation[8].

5 operating condition points specified at rational speed of 1750 r/min are selected as shown in table 1.

Table 1. Different operating condition points.

	Point 1	Point 2	Point 3	Point 4	Point 5
Flow rate (m^3/h)	14000	16000	18000	20000	22000

3. Results

3.1. Theoretical calculation of total pressure and total pressure efficiency

According to GB1236-2000, the fan total pressure is defined as the sum of static pressure difference and axial dynamic pressure difference between inlet and outlet of the fan. The rotary dynamic pressure isn't taken account of in the calculation of total pressure[9]. The calculation formula is

$$p_t = p_{st2} - p_{st1} + \frac{1}{2}\rho\left[\left(\frac{q_v}{A_2}\right)^2 - \left(\frac{q_v}{A_1}\right)^2\right] \quad (1)$$

The calculation formula of fan power N is

$$N = T \cdot n \times \frac{2\pi}{60} \quad (2)$$

The calculation formula of total pressure efficiency η_t is

$$\eta_t = \frac{q_v \cdot P_t}{N} \quad (3)$$

In the formula, p_{st2} and p_{st1} is the static pressure of outlet flow and inlet flow of the fan respectively. As fan outlet is directly connected with atmosphere, the outlet static pressure equals to zero. ρ is air density and q_v is volume flow rate. A_2 and A_1 is outlet area and inlet area of the fan respectively. According to the stand, 'the fan outlet area shall be taken as the gross area at the outlet flange or the outlet opening in the casing without deduction for motors, fairings or other obstructions', so A_2 is the difference value of cross-sectional area between airway and shaft and equals to 0.375m^2, A_1 is the cross-sectional area of airway and equals to 0.386m^2.

3.2. Effects of shaft supporting structure on inlet and outlet pressure

Based on the structure shown in figure 2, the flow field in the test device is calculated by using FLUENT. Changing the distance L and then analysing the pressure distribution to obtain a proper distance at which the obstruction has negligible influence on the outlet pressure of axial-flow fan. The value of L is set as 50mm, 70mm and 100mm. For the purpose of comparison, the pressure distribution is also calculated without any supporting structure.

Figure 5 is the contours of static pressure in vertical section and axial cross section of the outlet with flow rate of 22000m^3/h in the airway of 700mm in diameter.

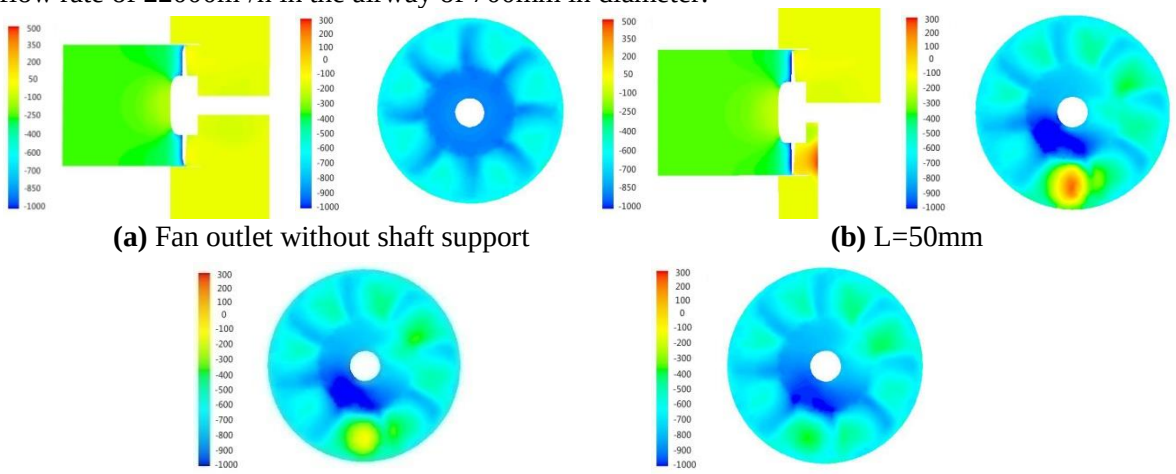

(a) Fan outlet without shaft support **(b)** L=50mm

(c) L=70mm **(d)** L=100mm

Figure 5. Contours of static pressure.

It can be seen from figure 5 that, when L=50mm, the dynamic pressure of airflow transforms into static pressure as obstructed by the supporting structure, which makes the static pressure at the bottom area of outlet section increases obviously. Meanwhile, performance property of the impeller remains the same, thus making the inlet static pressure increase correspondingly. However, the outlet static pressure equals to zero according to the standard, so the increased value of outlet static pressure isn't taken account of in the calculation of total pressure. According to formula (1), p_{st2} remains unchanged and p_{st1} increases, making the test value of total pressure below the actual value. As L increases, the outlet static pressure reduces gradually. When L=100mm, we can see from figure 4(a) in comparison with 4(d) that the outlet static pressure still rises with the influence of supporting structure, but the value is not very large. Therefore, it can be seen that the outlet obstruction doesn't influence the measurement of total pressure when L is greater than 100mm in this device.

However, the shaft rigidity may not meet requirements when the supporting structure is too far from the fan outlet, so the shaft rigidity and the influence of obstruction are considered together to improve the design of supporting structure. As shown in figure 6, the supporting structure is far from the outlet with a wedge-shaped axial stiffened plate to guarantee the rigidity of shaft. The distance between

stiffened plate and fan outlet equals to 50mm, which remains consistent with the original design. The distance between motor base and fan outlet equals to 280mm, which is obtained through trial and error.

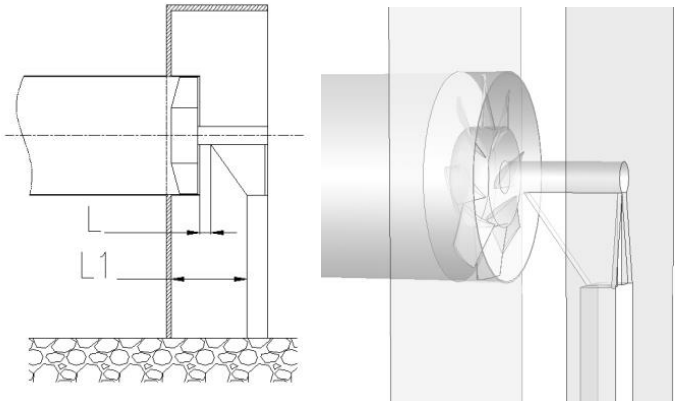

Figure 6. 3-D model of computational domain after improvement of supporting structure.

Similarly, figure 7 is the contours of static pressure in vertical section and axial cross section of the outlet with flow rate of 22000m^3/h. Compare figure 5(a) and 5(d) with figure 7, we can see that improved structure has little influence on outlet pressure when the distance is 280mm.

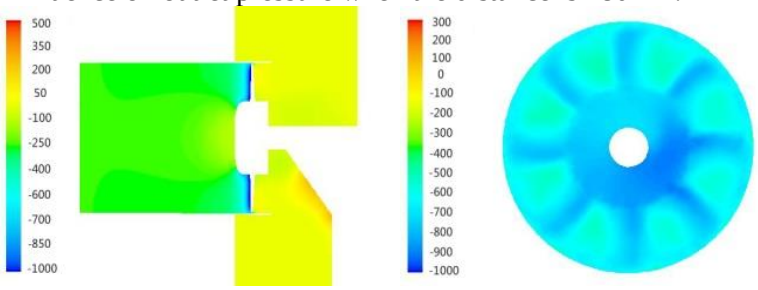

Figure 7. Contours of static pressure after improvement of supporting structure.

3.3. Effects of shaft supporting structure on total pressure efficiency

Figure 8 is the comparison chart of total pressure efficiency versus flow rate at different distances of supporting structure shown in figure 2. As L increases, total pressure efficiency of the fan is getting closer to the value when the fan outlet is not obstructed, and with the increase of flow rate, the influence of obstruction on total pressure efficiency becomes greater. When L=100mm, total pressure efficiency is very close to the value of no obstruction, and a larger distance may lead to an even better coincidence. To meet the requirement of rigidity, the extension length of the shaft shouldn't be too big, and the comparison of total pressure efficiency with different supporting structures is shown in figure 9. We can see that the fan total pressure efficiency with the wedge-shaped supporting structure is very close to the value without any supporting structure, and its obstruction effect can be neglected approximately. Through simulation, it's shown that the improved supporting structure can ensure the shaft rigidity and have little influence on the pressure distribution at the fan outlet at the same time.

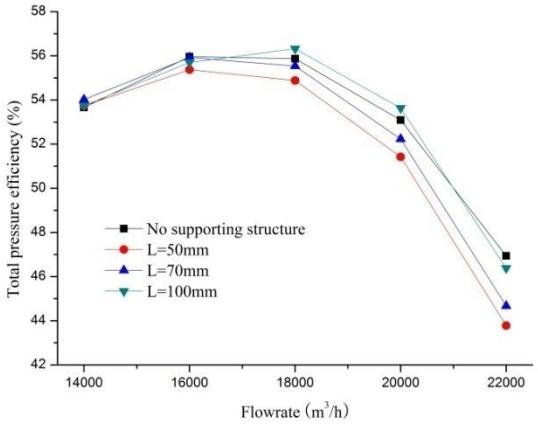

Figure 8. η-Q curves at different distances between supporting structure and fan outlet.

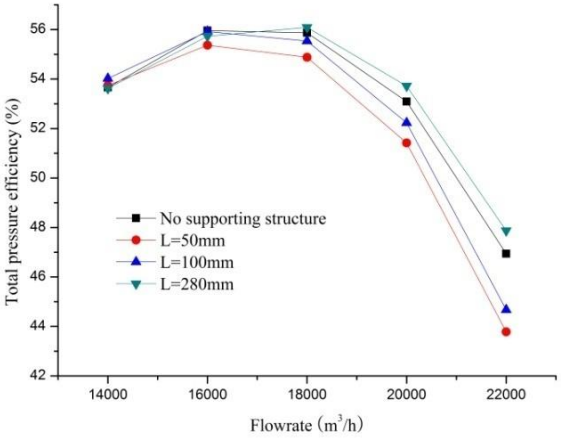

Figure 9. η-Q curves after improvement of supporting structure.

4. Conclusions

- For the performance test of an axial-flow fan conducted in a type-C ducted inlet device, if the shaft supporting structure is too close to the fan outlet, the test values of total pressure and total pressure efficiency decrease.
- Under the premise of ensuring the rigidity of connecting shaft, we can properly increase the distance between supporting structure and fan outlet, which may decrease the influence of obstruction on test results.

5. Acknowledgment

This work was supported by the National Natural Science Foundation of China (grant number 512754 52).

6. References

[1] GB/T1236-2000 2001 *Industrial fans - Performance testing using standardized airways*. （Beijing：Standards Press of China).

[2] Li J F, Lv J F. 2006 Simulation of air flow in a blower fluid machinery, **34(4)**：11-13.

[3] Chang Z Z, Luo H. 2009 Application of CFD software in the design of fan. *Compressor,*

Blower and Fan Technology, **(2)**, 60-64.
[4] Liu S, Wu S F, Zhang L X. 2009 Discussion of 3-D modeling for axial-flow fan and its internal flow field based on CFD. *Compressor, Blower and Fan Technology*, **(2)**, 16-19.
[5] Shangguan W B, Wu M, Wang Y Y. 2010 Calculation method of aerodynamic performances of engine cooling fans. *Automotive Engineering*, **32(9)**:800-802.
[6] Liu Y, Zheng S Y, Shen H T. 2013 Effects of airfoil thickness on performances of axial-flow fan. *Compressor, Blower and Fan Technology*, **(2)**, 15-18.
[7] Ashcroft G, Nurnberger D.2009 A computational investigation of broadband noise generation in a low-speed axial fan. *Proceedings of the 15th AIAA/CEAS Aeroacoustics Conference*, AIAA-2009-3219, 2009.
[8] Zhu Z Q. 1998 Computational fluid dynamics. (Beijing: Beihang University Press).
[9] Wu Y L, Chen Q G, Liu S H. 2011 Fans and Compressors.（Beijing：Tsinghua University Press）.